Terahertz Hall measurements on optimally doped single-crystal $Bi_2Sr_2CaCu_2O_{8+x}$

G. S. Jenkins,[1] D. C. Schmadel,[1] A. B. Sushkov,[1] G. D. Gu,[2] H. Kontani,[3] and H. D. Drew[1]
[1]*Center for Nanophysics and Advanced Materials, Department of Physics, University of Maryland, College Park, Maryland 20742, USA*
[2]*Condensed Matter Physics & Materials Science Department, Brookhaven National Laboratory, Upton, New York 11973-5000, USA*
[3]*Department of Physics, Nagoya University, Furo-cho, Nagoya 464-8602, Japan*
(Received 26 June 2010; published 24 September 2010)

The infrared Hall angle in optimally doped single-crystal $Bi_2Sr_2CaCu_2O_{8+x}$ was measured from 3.05 to 21.75 meV as a continuous function of temperature from 25 to 300 K. In the normal state, the temperature dependence of the real part of the cotangent of the infrared Hall angle obeys the same power law as dc measurements. The measured Hall frequency ω_H is significantly larger than the expected value based on angular-resolved photoemission spectroscopy data analyzed in terms of the relaxation-time approximation. This discrepancy as well as the temperature dependence of Re(cot θ_H) and ω_H is well described by a Fermi-liquid theory in which current vertex corrections produced by electron-magnon scattering are included.

DOI: 10.1103/PhysRevB.82.094518 PACS number(s): 74.72.−h, 78.20.Ls, 71.18.+y, 71.10.Ay

I. INTRODUCTION

Ever since the discovery of high-T_c cuprate superconductors, Hall angle measurements have figured prominently in the discussion of two broad classes of theoretical approaches of the nonsuperconducting state: Fermi-liquid and non-Fermi-liquid descriptions. The cotangent of the dc-Hall angle in optimally doped p-type cuprates exhibits an anomalous, nearly quadratic temperature dependence[1–5] while the longitudinal resistivity shows a linear dependence over a wide range of temperature.[5] The measured dc-Hall coefficient R_H near the superconducting transition temperature T_c is a factor of 3–4 larger[1–4] than that predicted by Luttinger's theorem while angular-resolved photoemission spectroscopy (ARPES) measurements show a reasonably simple large holelike Fermi surface (FS) whose area is consistent with the stoichiometric doping (although there are some subtleties associated with the bilayer splitting in double-layer compounds).[6] These facts have often been interpreted as proof of distinctly non-Fermi-liquid behavior spurring the development of novel and exotic theories to describe the phenomenology.[7,8]

However, recent Shubnikov de Haas and de Haas van Alphen (dHvA) measurements have demonstrated sharp oscillations in $1/H$ in both overdoped and underdoped p-type cuprates,[9–13] a hallmark signature of quantum oscillations and the existence of a well-defined Fermi surface and attendant quasiparticles. In overdoped $Tl_2Ba_2CuO_{6+\delta}$ (Tl-2201),[13] the area of the FS as deduced from dHvA oscillations is consistent with ARPES measurements,[14] angular magnetoresistance oscillations (AMROs) measurements,[15] low-temperature Hall coefficient measurements,[16] and Luttinger's theorem.[14] There is general agreement between ARPES and band-structure calculations.[17,18] Importantly, the Wiedemann-Franz law has been experimentally verified.[17,19] This evidence appears to validate Fermi-liquid theory (FLT) at least in the strongly overdoped p-type cuprates.

Underdoped p-type cuprates exhibit more complicated behavior. Measured in zero field at temperatures above T_c, the FS depicted by ARPES shows disconnected gapless Fermi arcs that have holelike curvature[6] whose length diminishes with decreasing doping and temperature.[20] In high field and low temperature, dc-R_H measurements show a negative electronlike behavior[21] while the measured frequency of quantum oscillations in $1/H$ imply a drastically smaller FS than the large holelike FS implied by ARPES. The measured value of the cyclotron mass in underdoped systems, $m_c \sim 3m_e$,[9–12] is very near the band value associated with the full FS. Generally for a small FS, one would expect a large variation in the energy dispersion resulting in a much reduced cyclotron mass.

Quantum oscillation experiments have not been successfully performed on optimally doped material since relatively short lifetimes and the present limit of achievable magnetic fields conspire to make measurements untenable. This is unfortunate since, ideally, one would like to directly compare quantum oscillation, ARPES, low frequency optical Hall, and other dc-transport measurements. Since infrared (IR) Hall measurements do not suffer from the strict constraints like those imposed on quantum oscillation experiments, they have been performed on $YBa_2Cu_3O_{6+x}$ (YBCO-123) thin films at various doping levels at ~100 meV in low fields (~8 T) above T_c, circumstances more like the zero-field ARPES conditions than the high-field quantum oscillations experiments. The IR Hall frequency is holelike and increases with decreasing doping, a signature of FS reconstruction consistent with formation of small pockets.[22] However, the relatively high frequency of the reported IR Hall measurements complicate direct comparisons with ARPES measurements due to known intermediate energy scales such as the high-energy renormalization of the dispersion as measured by ARPES,[6] interband transitions,[23] the pseudogap energy,[24] and magnetic correlations measured by neutron experiments.[25] Furthermore, the Cu-O chain contribution to the longitudinal conductivity uniquely associated with YBCO-123 complicates the analysis of the IR Hall data making direct quantitative comparisons difficult.

IR Hall measurements at low frequencies ($\lesssim$10 meV) below these characteristic energy scales directly probe the intrinsic properties of the FS in a unique way. This technique, together with quantitative comparisons with ARPES and

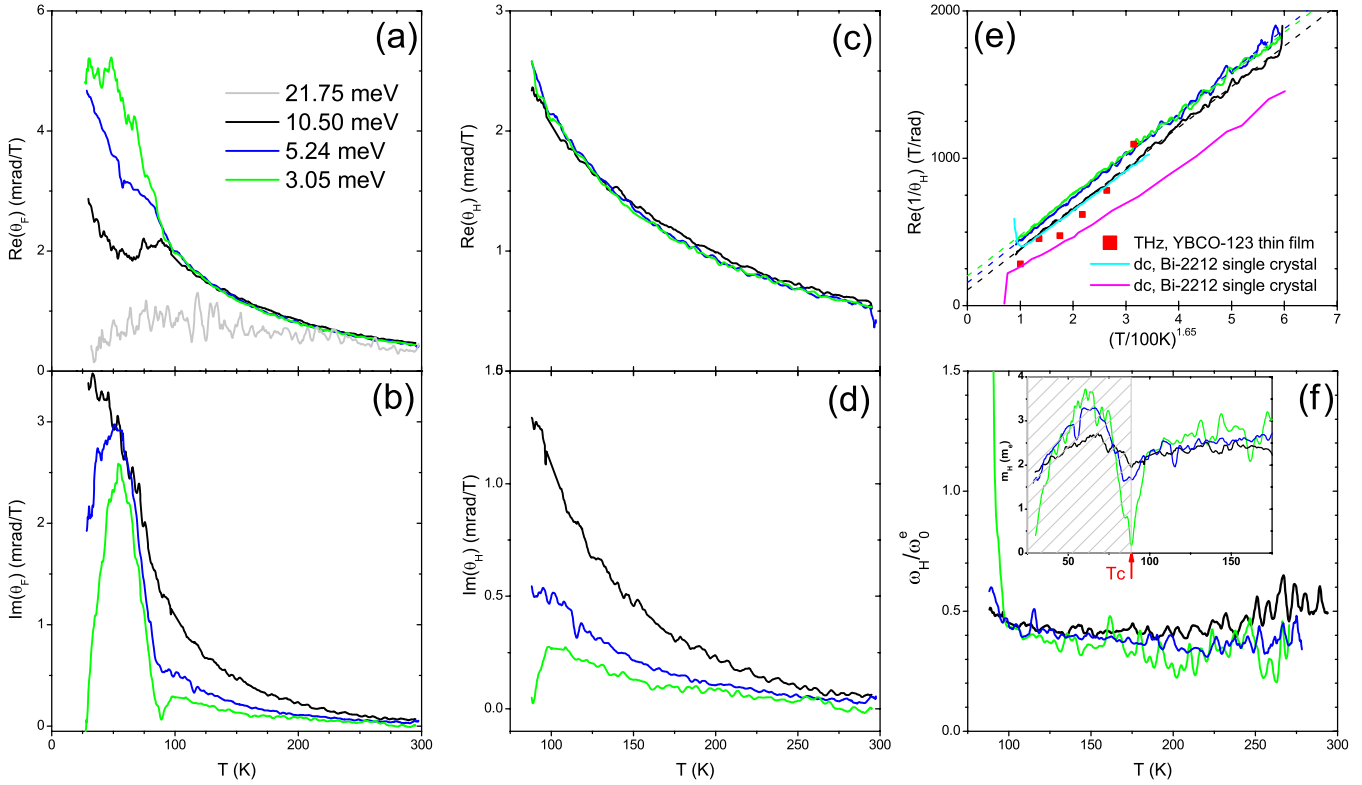

FIG. 1. (Color online) (a) and (b) Real and Imaginary parts of the Faraday angle measured at 3.05, 5.24, 10.5, and 21.75 meV. The imaginary part of the Faraday angle for the 21.75 meV data set was not reliably measured so is not reported. (c) and (d) Real and imaginary part of the Hall angle in the normal state. (e) $\mathrm{Re}(1/\theta_H)$ measurements are consistent with THz measurements in the range 0.41–1.24 meV performed on optimally doped YBCO-123 films (red squares) (Ref. 36) as well as dc-cot θ_H measurements performed on slightly overdoped (T_c=86.5 K) (cyan) (Ref. 4) and optimally doped single-crystal Bi-2212 (violet) (Ref. 3). The dashed straight lines are linear fits to the IR Hall data. (f) The measured Hall frequency normalized to the free-electron Hall frequency, ω_0^e=0.115 meV/T. The inset shows the Hall mass in units of bare electron mass m_e versus temperature. The superconducting state is cross hatched in gray since the single-fluid Drude parametrization does not apply to the superconducting state.

other transport data, have proven very successful in affirming the causal mechanism of the extremely anomalous behavior of the Hall effect in *n*-type cuprates in the overdoped regime[26,27] as well as the underdoped regime in the paramagnetic state.[28] Furthermore, the technique has proven a reliable and sensitive probe of FS reconstruction as established in underdoped *n*-type cuprates below the Néel temperature,[29,30] manifesting as a drastically reduced Hall mass.[28]

In this paper, we report finite frequency Hall angle measurements on optimally doped $Bi_2Sr_2CaCu_2O_{8+x}$ (Bi-2212) single crystals in the terahertz (THz), or far IR (FIR), spectral region. The FIR Hall response is significantly larger than expected based on ARPES results analyzed within the relaxation-time approximation (RTA), a result similar to dc-Hall measurements. This discrepancy can be accounted for by including current vertex corrections (CVCs) produced by electron-magnon scattering in a Fermi-liquid-based theoretical analysis, a mechanism which is notably supported in *n*-type cuprates.[26–28]

II. EXPERIMENTAL DESCRIPTION

Optimally doped single-crystal $Bi_2Sr_2CaCu_2O_{8+x}$ grown by the traveling floating-zone method[31] were exfoliated normal to the *c* axis and mounted to a *z*-cut quartz substrate with a broadband nichrome antireflection coating.[32–35] The thickness was determined to be 100 nm with an area defined by a 2.5 mm diameter circular aperture. A midpoint T_c of 87 K with a width of 1.5 K was measured using an ac magnetic susceptibility probe. As discussed later in Sec. VIII, precursive superconductivity behavior exhibited up to temperatures as high as 100 K suggests that the sample is not overdoped.

The Faraday rotation and circular dichroism (expressed as the complex Faraday angle, $\theta_F = t_{yx}/t_{xx}$, the ratio of the off-diagonal and diagonal Fresnel transmission amplitudes) as well as the relative transmission were measured at a set of discrete frequencies as a continuous function of temperature. The output of a far-infrared molecular vapor laser was polarization modulated via a rotating quartz quarterwave plate and subsequently transmitted through the *c*-axis-oriented sample at normal incidence in applied magnetic fields up to 8 T. The complex Faraday angle was obtained by harmonically analyzing the detector signal, a technique that is detailed elsewhere.[32] Both the real and imaginary parts of the Faraday angle measured at fixed temperature were linear in applied field. The Faraday angle as a continuous function of temperature is presented in Figs. 1(a) and 1(b). The imaginary part of the Faraday angle measured at 21.75 meV could not reliably

be measured due to particularly low optical throughput power.

In the normal state, the complex Hall angle is derived from the Faraday angle in the thin-film limit via $\theta_H=(1+\frac{n+1}{Z_0\sigma_{xx}d})\theta_F$, where σ_{xx} is the longitudinal conductivity, n is the index of refraction of the quartz substrate, Z_0 is the impedance of free space, and d is the thickness of the film.[32] Fourier transform infrared (FTIR)-spectroscopic transmission measurements were performed in the spectral range from 2 to 25 meV at a set of discrete temperatures ranging from 100 to 300 K. The complex conductivity σ_{xx} was extracted by fitting to a simple Drude form. θ_H is very insensitive to errors in σ_{xx} since the conversion factor was found to be $<15\%$ at all measured frequencies and temperatures.[33]

The resulting normal-state complex Hall angle measured at 3.05, 5.24, and 10.5 meV as a function of temperature is shown in Figs. 1(c) and 1(d). Both the real and imaginary parts of the Hall angle at all temperatures and frequencies are positive indicating a net holelike Hall response.

III. NORMAL-STATE DATA ANALYSIS: DRUDE MODEL

Large linewidths of the spectral function are observed by ARPES in optimally doped cuprates in the normal state.[6,37–45] Even though the Landau's FLT required quasiparticles with an energy greater than their inverse lifetime, the many-body perturbation theory which validated the original FLT does not. This approach has lead to the concept of the marginal FLT in the cuprates.[8] In general the presence of inelastic scattering has lead to the so-called extended Drude model in which the mass and scattering rate are renormalized by a frequency- and temperature-dependent self-energy. The predictions of FLT are examined in Secs. IV–VI in optimally doped Bi-2212 in terms of the quasiparticle self-energy as interpreted by ARPES measurements.

Spectroscopic measurements on optimally doped cuprates show that the longitudinal conductivity is well described by a Drude model in the FIR where the scattering rate is proportional to temperature and the plasma frequency is temperature independent[46,47] consistent with early ARPES measurements[37] and dc resistivity measurements.[46] Kontani[27] and others[48] have shown that many-body perturbation theory can account for σ_{xx} giving some justification for the application of an extended Drude model. At terahertz frequencies and temperatures above T_c, the frequency dependence of the self-energies can be ignored resulting in a Landau parameter which is only temperature dependent. In this case the extended Drude model becomes equivalent to a Drude model with a temperature-dependent mass and relaxation rate.

Motivated by these experimental results and ideas of the broader applicability of FLT, we analyze our FIR Hall results in terms of a Drude parametrization. It should be noted, however, that the well-known anomalous Hall effect[1] where dc-cot $\theta_H\sim T^{1.78}$ together with the dc resistivity $\sim T$ is difficult to reconcile within a Drude parametrization. One of the motivations for extending dc-Hall angle measurements to THz frequencies was to separately determine the temperature dependences of the Hall scattering rate and the Hall mass.

Within a Drude parameterization, $\tan\theta_H\approx\theta_H=\omega_H/(\gamma_H-i\omega)$ where $\omega_H=eB/cm_H$ is the Hall frequency, m_H is the Hall mass, γ_H is the Hall scattering rate, ω is the applied optical frequency, B is the applied magnetic field, c is the speed of light, and e is the bare charge of an electron. Rearranging, we may write

$$\mathrm{Re}(1/\theta_H)=\gamma_H/\omega_H,$$

$$\frac{\omega_H}{\omega_0^e}=-\frac{\omega}{\omega_0^e}\mathrm{Im}(1/\theta_H)^{-1}, \tag{1}$$

or, equivalently, expressing the Hall frequency in terms of the Hall mass gives

$$\frac{m_H}{m_e}=-\frac{\omega_0^e}{\omega}\mathrm{Im}(1/\theta_H), \tag{2}$$

where $\cot\theta_H\approx 1/\theta_H$, $\omega_0^e=0.115$ meV/T is the bare electron cyclotron frequency and m_e is the bare electron mass. Figures 1(e) and 1(f) show $\mathrm{Re}(1/\theta_H)$, ω_H, and m_H at several FIR frequencies as a function of temperature.

ω_H (and m_H) is frequency independent (within the errors of the measurement) and only slightly temperature dependent. As temperature increases or frequency decreases, the ω_H data become more noisy commensurate with the decreasing magnitude of the Hall angle. The best signal to noise for determining the temperature dependence of ω_H are the 10.5 and 5.24 meV data sets which show a very discernible bowed behavior.

Even at finite frequencies up to 10.5 meV, $\mathrm{Re}(1/\theta_H)$ obeys a power law $\sim T^{1.65\pm0.1}$ consistent with published THz Hall measurements performed on optimally doped YBCO-123 films at 0.41–1.24 meV (Ref. 36) and dc measurements performed on Bi-2212 single crystals[3,4] and films.[1] Although the temperature power laws are the same, varying offsets between data sets are presumably from variations in sample quality and associated impurity scattering. A small frequency dependence is discernible which shows $\mathrm{Re}(1/\theta_H)$ decreasing slightly with increasing frequency consistent with earlier FIR broadband measurements on optimally doped YBCO-123 near T_c.[49]

The Drude analysis is easy to understand but very limited. It assumes that two parameters, a characteristic frequency and scattering rate, can reasonably capture the physics of all transport measurements. However, Fermi surfaces which have anisotropic scattering rates and Fermi velocities will manifest as differing effective Drude parameters when probed with various experimental techniques due to the nature of averaging around the FS. In order to compare the IR Hall data with ARPES and other transport data, we review Boltzmann formalism.

IV. BOLTZMANN THEORY: TRANSPORT AND ARPES DATA COMPARISONS

Within the RTA in Boltzmann theory, the off-diagonal and diagonal conductivities may be expressed as path integrals around the FS involving the Fermi velocity, scattering rate, and size and shape of the FS,[48]

$$\sigma_{xy}=\frac{e^2}{hc_0}\frac{e\vec{B}}{\hbar c}\oint_{\mathrm{FS}}dk\frac{\vec{v}_k^*\times d\vec{v}_k^*/dk}{(\gamma_k^*-i\omega)^2},$$

$$\sigma_{xx} = \frac{e^2}{hc_0} \oint_{\mathrm{FS}} dk \frac{|\vec{v}_k^*|}{\gamma_k^* - i\omega}, \tag{3}$$

where v_k^* is the (renormalized) Fermi velocities as measured by ARPES, $\gamma_k^* = v_k^* \Delta k$, Δk is the momentum distribution curve (MDC) width as measured by ARPES, and c_0 is the average interplane spacing. Various transport quantities can be calculated but the relevant quantities of interest are the dc-Hall coefficient $R_H = \sigma_{xy}/\sigma_{xx}^2$, the Hall angle $\theta_H = \sigma_{xy}/\sigma_{xx}$, and the Hall frequency and scattering rate given by the expression $\omega_H/(\gamma_H - i\omega) = \sigma_{xy}/\sigma_{xx}$.

In a comparison of ARPES and transport data it is important to recognize that the current relaxation time that characterizes transport is not necessarily the same as the quasiparticle lifetime measured by ARPES. For example, small-angle elastic scattering does not affect transport but does contribute to MDC width broadening.[48] However, it is equally important to realize that for the rather simple Fermi surfaces under consideration in this study, R_H and ω_H (and m_H) depend only weakly on the anisotropy of the scattering rate. In the limit of high frequency or isotropic scattering, R_H (Ref. 50) and ω_H are independent of scattering rate, and are given by

$$\omega_H = \frac{e\vec{B}}{\hbar c} \frac{\oint_{\mathrm{FS}} \vec{v}_k^* \times d\vec{v}_k^*}{\oint_{\mathrm{FS}} dk |\vec{v}_k^*|},$$

$$R_H = \frac{hc_0}{e^2} \frac{e\vec{B}}{\hbar c} \frac{\oint_{\mathrm{FS}} \vec{v}_k^* \times d\vec{v}_k^*}{\left(\oint_{\mathrm{FS}} dk |\vec{v}_k^*|\right)^2}. \tag{4}$$

Note that for the case of isotropic mean-free path, v_k^*/γ_k^*, and a single sign of concavity associated with the entire FS, the dc-Hall coefficient is given by $R_H = R_H^{Lut}(C/C')^2$, where C and C' are the circumferences of a circular and noncircular Fermi surface of the same area, and R_H^{Lut} is the Luttinger value of the Hall coefficient.

The cyclotron frequency ω_c (or cyclotron mass m_c) is inherently independent of scattering rate and depends only on the Fermi velocity and circumference of the FS,

$$\frac{\omega_c}{\omega_0^e} = \left(\frac{m_c}{m_e}\right)^{-1} = m_e \frac{eB}{\hbar c} \frac{2\pi}{\oint_{\mathrm{FS}} \frac{dk}{|\vec{v}_k^*|}}, \tag{5}$$

where ω_0^e is the free-electron cyclotron frequency and m_e is the bare electron mass. The Hall frequency is exactly equal to the cyclotron frequency in the special case of a circular FS with isotropic velocity and isotropic scattering.

V. SUBSTANTIATING COMPARISONS BETWEEN ARPES +RTA AND TRANSPORT IN CUPRATE SYSTEMS

ARPES measurements reflect the bulk band dispersion and FS topology in various cuprate systems. In overdoped $Pr_{2-x}Ce_xCuO_4$ (PCCO) in the $T \to 0$ limit, the measured dc-R_H agrees with the value calculated from ARPES data within the RTA, and both are consistent with Luttinger's theorem.[26] In underdoped n-type cuprates, the number density of the electron pocket derived from ARPES measurements is consistent with the stoichiometric doping as measured in $Sm_{1.86}Ce_{0.14}CuO_4$ (Ref. 29) and $Nd_{2-x}Ce_xCuO_{4\pm\delta}$.[28,51,52] In optimally doped Bi-2212, the band dispersion as measured by recent low-energy laser ARPES agrees with earlier higher energy measurements verifying that both techniques are measuring bulk properties.[43]

Before analyzing Bi-2212, it is instructive to compare ARPES and transport data in strongly overdoped Tl-2201 where deviations away from simple Fermi-liquidlike behavior are much less severe. The ARPES measured FS size from reported data is reasonably consistent with the de Haas van Alphen measurements,[13] AMRO measurements,[17] Luttinger's theorem,[14,53] and low-temperature Hall coefficient measurements.[16] There is general agreement between ARPES and band-structure calculations,[17,18] and the Wiedemann-Franz law has been experimentally verified.[17,19]

These results make a compelling case for the applicability of Fermi-liquid theory in strongly overdoped p-type cuprates. We directly test the relaxation-time approximation by using Boltzmann transport theory to calculate dc-R_H [Eq. (3)] and m_c [Eq. (5)] with parameters derived from ARPES data. The size and shape of the FS are given by the following tight-binding parameters: $\mu = 0.2438$, $t_1 = -0.725$, $t_2 = 0.302$, $t_3 = 0.0159$, $t_4 = -0.0805$, and $t_5 = 0.0034$, all expressed in electron volts.[14] The scattering rate as a function of angle around the FS is reported.[14] The nodal and antinodal Fermi velocities are given by $v_{\pi,\pi} = 2.0 \pm 0.15$ eV Å and $v_{\pi,0} = 0.765$ eV Å, respectively.[54] Interpolation between the nodal and antinodal Fermi velocities is reasonably provided by the tight-binding model. However, to conservatively estimate errors in the interpolation, a range of functional forms of the Fermi velocity given by $v_k = v_{\pi,\pi} + (v_{\pi,0} - v_{\pi,\pi})(\sin 2\theta)^n$ are used where n ranges from 2 to 8 and the location on the FS is parameterized by the angle θ.

The integrated area of the ARPES measured FS yields a number density consistent with the Luttinger value associated with the stoichiometric doping, 1.26 holes/Cu atom. The Hall coefficient calculated from the stoichiometric number density yields $R_H = 8.4 \times 10^{-10}$ m^3/C, consistent with the low-temperature measurement of dc-$R_H = 8.5 \times 10^{-10}$ m^3/C.[16] However, the measured dc-R_H increases to a peak value of about 12×10^{-10} m^3/C at ~ 100 K and, importantly, falls off to a value of about 10×10^{-10} m^3/C at higher temperatures ~ 300 K.

Evaluating Eq. (3) yields a Hall coefficient in the range of 7.5×10^{-10} m^3/C to 10×10^{-10} m^3/C. The range of values results from the various functional forms assumed for the interpolated values of v_k^* as well as some errors introduced from uncertainties associated with the ARPES measured scattering rates. Good agreement between the ARPES +RTA value and the low-temperature dc-R_H value is achieved for the case where $n \approx 3$ for the velocity anisotropy interpolation function.

The measured dc-R_H value at 100 K lies well outside the range that is predicted by ARPES (assuming that the ARPES

measured velocity and scattering rate anisotropy do not change significantly between T_c and 100 K) illustrating that a breakdown of the simple relaxation-time approximation occurs for Tl-2201 at a doping of 1.26, even considering the conservatively large error bars. Therefore overdoped Tl-2201 appears to have an anomalous Hall effect similar to optimally doped p-type cuprates although it is much weaker.

At sufficiently high temperature, the scattering becomes dominated by phonon scattering and is expected to become isotropic. The Hall coefficient is then independent of scattering rate [see Eq. (4)]. Under the assumption of isotropic scattering and Fermi velocities which agree with ARPES measurements, the predicted ARPES value of the Hall coefficient is $9.5 \pm 0.5 \times 10^{-10}$ m^3/C in reasonable agreement with the dc-R_H value of about 10×10^{-10} m^3/C at 300 K. Whatever the cause of the anomalous dc-Hall effect in overdoped Tl-2201, the effect seems to disappear at low temperature and in the vicinity of room temperature. At very high temperature in other cuprate systems, the Hall coefficient continues to decrease due to thermally activated transitions to other bands.[23,55]

For completeness, it should be noted that under the assumptions of isotropic mean-free path, the Hall coefficient found from integrating the nearly circular FS yields the Luttinger value as expected which is consistent with the dc measured value at low temperature. However, the ARPES data shows that neither isotropic scattering rate nor isotropic mean-free path occurs at low temperature.

The cyclotron mass m_c calculated from Eq. (5) ranges from $4.5m_e$ to $5.7m_e$, a result consistent with quantum oscillations measurements where $m_c = 4.1 \pm 1.0$.[13] The associated error bars are large for both the ARPES+RTA value as well as the measured value. If a more accurate m_c is measured by quantum oscillation experiments and more ARPES velocities are measured so as to derive the functional form of the velocity around the FS, a more thorough comparison could be made.

The Tl-2201 case substantiates the ARPES+RTA methodology for the hole-doped cuprate systems while concurrently showing an interesting breakdown of the RTA in the vicinity of 100 K, even in the strongly overdoped regime. As we show in the next section, the discrepancy between dc-R_H and the ARPES+RTA value is much larger in optimally doped Bi-2212 than for strongly overdoped Tl-2201 but both show an enhanced Hall response above the ARPES+RTA value. Importantly, the IR Hall response also shows an enhancement above the ARPES+RTA value.

VI. BI-2212: HALL DATA COMPARISON WITH ARPES +RTA

There are complications which arise when comparing Bi-2212 ARPES results to transport data. The nodal region is very well characterized but intracell bilayer coupling complicates the analysis in the vicinity of the antinode. Recent ARPES measurements have resolved the bilayer splitting in optimally doped Bi-2212.[39,42] Early measurements reported an anisotropy in the scattering rate of 2–3 between the nodal and antinodal points[37] but they were not resolving the bilayer splitting. It has been well argued that these early ARPES measurements on Bi-2212 grossly overestimated the scattering rate away from the nodal direction due to the unresolved bilayer splitting.[6,45]

However, as we will demonstrate, the dc- and FIR Hall response is much larger than the ARPES+RTA prediction. Effects produced by bilayer splitting and anisotropic scattering are small compared to this discrepancy, and both effects when fully taken into account tend to *increase* the discrepancy.

We begin our analysis by assuming an isotropic scattering rate but consider anisotropic scattering effects later. An isotropic Fermi velocity with a large holelike FS was measured by ARPES.[37,38] The Fermi velocity was measured to be about 1.8 eV Å at 100 K.[37,40,41] The shape of the FS is given by a tight-binding model where the dispersion is given by $\epsilon_p = -2t_1(\cos p_x + \cos p_y) + 4t_2 \cos p_x \cos p_y - 2t_3(\cos 2p_x + \cos 2p_y)$ with hopping parameters $t_1 = 0.38$ eV, $t_2 = 0.32t_1$, and $t_3 = 0.5t_2$ (Refs. 52, 56, and 57) and a chemical potential chosen such that the area of the FS is commensurate with Luttinger's theorem. This model was modified to include bilayer splitting consistent with ARPES measurements on optimally doped Bi-2212 by adding a gap function given by $\Delta_0(\cos p_x x + \cos p_y y)^2$, where $\Delta_0 \approx \pm 50$ meV.[39,42] Under the assumptions of isotropic scattering and isotropic Fermi velocity (assuming the ARPES value of 1.8 eV Å) for the case where bilayer splitting is ignored (setting $\Delta_0 = 0$), we find $\omega_{H0} = \omega_{c0} = 0.33\omega_0^e (m_{H0} = 3.0m_e)$, where $\omega_0^e = 0.115$ meV/T is the free-electron cyclotron frequency, and dc-$R_{H0} = 5.8 \times 10^{-10}$ m^3/C. The deviation from the Luttinger value of dc-$R_H = 6.0 \times 10^{-10}$ m^3/C is due to the slightly noncircular FS.

If the velocity anisotropy given by the tight-binding dispersion for the $\Delta_0 = 0$ case are assumed (where the nodal velocity is scaled to the ARPES measured value of 1.8 eV Å), then it is found that deviations from the above calculated transport values are very small. The reason is that the tight-binding model shows only a slight anisotropy of the Fermi velocity where the nodal and antinodal velocities are approximately equal with a slight depression of about 15% in between.

When we include the bilayer splitting where $\Delta = +50$ meV (-50 meV) which changes the dispersion away from the nodal point (causing larger anisotropic variation in the Fermi velocity) as well as the size and shape of the Fermi surface, we find a suppression of the Hall frequency $\omega_H/\omega_0^e = 0.29(0.32)$, a cyclotron frequency of $\omega_c/\omega_0^e = 0.25(0.39)$, and a Hall coefficient of $R_H = 5.1 \times 10^{-10}$ m^3/C$(6.0 \times 10^{-10}$ m^3/C). The Boltzmann transport values predicted by ARPES including bilayer splitting are then $R'_{H0} = 5.5 \times 10^{-10}$ m^3/C, $\omega'_{c0} = 0.25\omega_0^e$, and $0.39\omega_0^e$ for the two Fermi surfaces, and $\omega'_{H0} = 0.30\omega_0^e$ (corresponding to $m'_{H0} = 3.3m_e$).

We introduce a scattering rate anisotropy of the form $\gamma(\theta) = 2 - \sin(2\theta)$ to the same tight-binding model such that the antinodal point scattering is twice as large as the nodal scattering, an overestimate of the anisotropy. For the $\Delta_0 = 0$ case, we find $R_{H0} = 7.8 \times 10^{-10}$ m^3/C, and ω_{H0} values ranging from $0.34\omega_0^e$ to $0.33\omega_0^e$ corresponding to the low- and high-frequency limits, respectively. If the bilayer splitting is

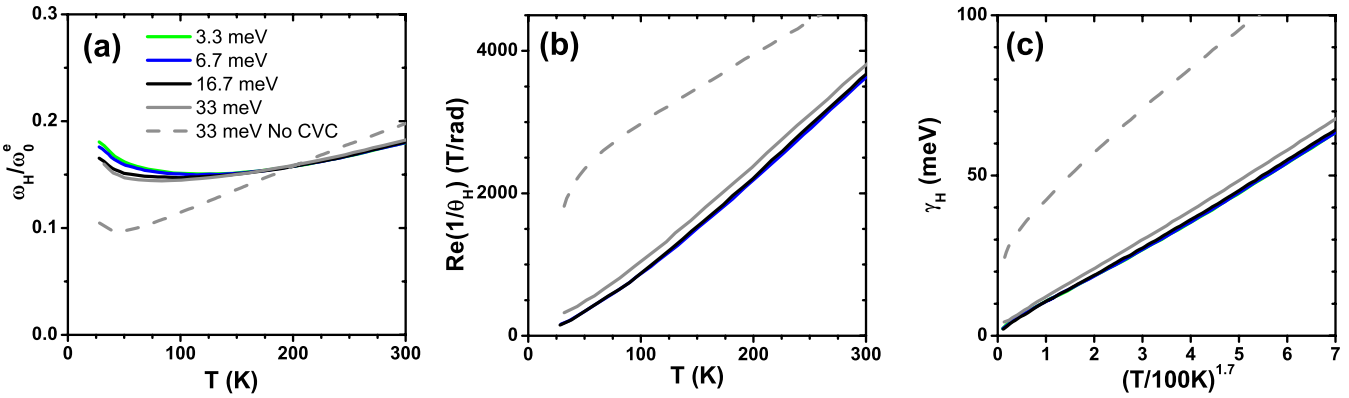

FIG. 2. (Color online) The calculated Hall angle using a FLEX+T-matrix approximation parameterized in the same manner as the reported data in Fig. 1 for easy comparison. Shown are graphs of the (a) Hall frequency ω_H normalized to the free-electron Hall frequency, ω_0^e=0.115 meV/T, (b) Re$(1/\theta_H)$, and (c) Hall scattering rate γ_H. The green (3.3 meV), blue (6.7 meV), and black (16.7 meV) plots in figures (b) and (c) are nearly indistinguishable.

then included while concurrently including the anisotropic scattering which is assumed to be the same in both the antibonding and bonding bands, then the values become $R_H'=7.4\times10^{-10}$ m^3/C and ω_H' ranges from $0.32\omega_0^e$ to $.30\omega_0^e$ between the low- and high-frequency limits, respectively.

Summarizing, using ARPES data for optimally doped Bi-2212,[6,37–45] R_H, ω_c, and ω_H (and m_H) were calculated within Boltzmann transport formalism. The ARPES+RTA value of $\omega_H=0.30\omega_0^e(m_H=3.3m_e)$ is substantially less than the measured value of $\omega_H=0.44\pm.04\omega_c^e$ at 100 K for all frequencies $\leq$10.5 meV. This represents a substantial enhancement of the FIR Hall response ~50% above the ARPES+RTA expectation. Similarly, the measured dc-R_H $\approx20\times10^{-10}$ m^3/C at 100 K (Refs. 1–4) is enhanced by a factor of 3–4 above the ARPES+RTA calculated value of $R_H=5.5\times10^{-10}$ m^3/C.

VII. COMPARISONS WITH FLEX+CVC MODEL

A theory of cuprate transport properties which includes electron-electron interactions mediated by antiferromagnetic fluctuations has been developed and extensively applied by Kontani.[27] Antiferromagnetic fluctuations were calculated within the fluctuation-exchange (FLEX) approximation, and the effective low-energy electron-electron interaction Hamiltonian is then proportional to the dynamical spin susceptibility. Electron-magnon scattering causes corrections to the self-energy as well as CVCs to the conductivity. CVCs change the magnitude of the k-dependent current and cause deviations of the current direction away from the FS normal. A T-matrix formalism has also been incorporated to account for superconducting fluctuation effects in the vicinity of T_c.

This theory has proven highly successful in accounting for the features of the anomalous behavior of the dc-Hall effect in both electron- and hole-doped cuprates as a function of doping and temperature. More recently it has been applied to the frequency dependence of hole-doped cuprates at mid-IR frequencies and electron doped cuprates at THz frequencies. The theory successfully accounted for the doping, temperature, and frequency dependence of the IR Hall data on overdoped electron-doped cuprates.[26,28]

Calculated results of the IR Hall response are shown in Fig. 2. The calculation considers a one-band Hubbard model for the copper-oxygen planes with tight binding parameters for YBCO-123 (which is similar to Bi-2212 except for the presence of the chain bands) with a Coulomb interaction characterized by an on site potential U. The hole doping is set by the chemical potential. The longitudinal and Hall conductivity are calculated as a function of temperature for several representative THz frequencies. The calculations are performed both including and ignoring CVCs. The later case is equivalent to the RTA within the FLEX approximation. To compare with the experimental data, Re$(1/\theta_H)$, ω_H, and γ_H are calculated from the conductivity tensor via the definition of the Hall angle and Eq. (1).

The qualitative behavior of ω_H and Re$(1/\theta_H)$ is consistent with the IR Hall data. Both ω_H and Re$(1/\theta_H)$ in Figs. 2(a) and 2(b) exhibit very little frequency dependence consistent with the data in Figs. 1(e) and 1(f). The slight upward bowing of ω_H with temperature and the superlinearity of Re$(1/\theta_H)$ is reproduced (although the power law is somewhat weaker).

Previously reported calculations of dc-R_H in Ref. 27, Figs. 19(i) and 19(iii), show a very large enhancement of dc-R_H above that predicted by the RTA (the "No CVC" case) consistent with the experimentally measured enhancements in optimally doped Bi-2212 above the ARPES+RTA predicted value calculated in the previous section.[1]

Similar to the dc-R_H case, the enhancements of the IR Hall response ω_H above that expected from the ARPES +RTA value is also quantitatively equal to the enhancements calculated by including CVCs. As shown in Fig. 2(a), the enhancement of ω_H by the inclusion of CVCs at 100 K and 33 meV is $\omega_H^{\mathrm{CVC}}/\omega_H^{\mathrm{NoCVC}}=1.3$. This is consistent with the enhancement of the experimental value at 100 K and 10.5 meV above the ARPES+RTA value, $\omega_H^{\mathrm{FIR}}/\omega_H^{\mathrm{ARPES+RTA}}=1.5$, where $\omega_H^{\mathrm{FIR}}=0.44\omega_0^e$ from Fig. 1(f), $\omega_H^{\mathrm{ARPES+RTA}}\approx0.30\omega_0^e$ (which includes bilayer splitting effects), and ω_0^e =0.115 meV/T is the free-electron cyclotron frequency. The smaller enhancement of ω_H at THz frequencies compared with that of dc-R_H is well reproduced by the theory.

The calculations capture all of the qualitative features of the data. This is an impressive success of the theory since the

frequency and temperature dependence of the Hall data, as well as the quantitative discrepancy with the ARPES+RTA value, places severe constraints on theories.

Although the similarities between the data of Figs. 1(e) and 1(f) and the calculated values of Figs. 2(a) and 2(b) are striking, there are some important discrepancies. In particular, the magnitude of ω_H differs from the experimental value.

To address this issue, we note that the FS resulting from the model calculation differs significantly from the FS as measured by ARPES in Bi-2212. The tight-binding model parameters are $t_1=0.35$ eV, $t_2=0.17t_1$, and $t_3=0.2t_1$. The chemical potential is set to achieve the correct FS area corresponding to the stoichiometric doping. For $U=0$, the FS is very similar to that measured by ARPES. However, for nonzero U the Fermi surface becomes distorted due to self-energy corrections. The FS distortions result in much more curvature of the Fermi surface in the antinodal regions and less curvature in the vicinity of the nodal regions [compare the measured FS from Refs. 39 and 42 with Fig. 2(a) of Ref. 58]. Since ω_H weights more heavily the higher curvature regions of the FS, which for Kontani's FS occurs near the lower velocity sections near the Van Hove singularity in the vicinity of the antinode, the calculated value of $\omega_H^{\mathrm{NoCVC}}$ is expected to be substantially lower than our calculated value $\omega_H^{\mathrm{ARPES+RTA}}$.

In view of these FS differences between the model calculation and that observed by ARPES, it is not surprising that the model $\omega_H^{\mathrm{NoCVC}}\approx .11\omega_0^e$ is about a factor of 3 smaller than the ARPES+RTA derived value of $\omega_H^{\mathrm{ARPES+RTA}}\approx 0.30\omega_0^e$ although these values, in principle, should match.

Similarly, the experimental value of $\omega_H^{\mathrm{FIR}}=0.44\omega_0^e$, is roughly a factor of 3 larger than the model value of $\omega_H^{\mathrm{CVC}}=0.15\omega_0^e$. Again the magnitude is off but, most importantly, the enhancement ratio is approximately correct such that $\omega_H^{\mathrm{CVC}}/\omega_H^{\mathrm{NoCVC}}\sim\omega_H^{\mathrm{FIR}}/\omega_H^{\mathrm{ARPES+RTA}}$.

These absolute magnitude comparisons are exacerbated by another factor not included in the conductivity calculations. Mott correlations associated with the Coulomb repulsion are expected to shift conductivity spectral weight from the low-energy Drude-type response to high energies $\omega>U$.[57] Moreover, the spectral weight associated with σ_{xy} is suppressed by a factor of $\sim$3 more than σ_{xx} as demonstrated by an analysis of the FIR and MIR Faraday measurements on Bi-2212.[34] Since these Mott correlation effects are not included in the model, one expects an additional level of overestimation of the calculated ω_H.

The results on Bi-2212 should be contrasted to our previous results in overdoped PCCO where the Hall frequency calculated from the FLEX+CVC theory is larger than our measured value as one would expect from the omitted effects of spectral weight renormalization due to Mott correlations from the theory.[26] The effects from FS distortions due to the Hubbard U are smaller for n-type cuprates as can be seen in Fig. 2 of Ref. 58. Since the FS is smaller, the portion near $(\pi,0)$ is further from the magnetic Brillouin zone and the Van Hove singularity. Therefore, reductions in the Fermi velocity due to the addition of the Hubbard U to the tight-binding model are much less severe resulting in less reduction in ω_H calculated within the RTA approximation.

The good agreement of the FLEX+CVC theory in accounting for the enhancements of the IR Hall response above that predicted by the ARPES+RTA value while reproducing the frequency and temperature dependence is significant evidence that current vertex corrections to the conductivity together with interactions mediated by magnetic fluctuations are the origin of the anomalous Hall effect in the cuprates, an important conclusion of this work. However, the task of removing some deficiencies of the theory remain such as incorporating a proper treatment of Mott correlations on the conductivity spectral weight and self-consistently determining the Coulomb U to produce the measured ARPES FS.

VIII. PRECURSIVE SUPERCONDUCTIVITY

In the inset of Fig. 1(f), a dip feature observed in m_H at 3.05 and 5.24 meV has an onset temperature well above T_c but is most pronounced at 3.05 meV. This appears to be precursive superconducting behavior well above the transition temperature. Various experiments have exhibited precursive superconducting behavior in the normal state in the high-T_c cuprates: microwave cavity,[59] Nernst effect,[60] specific heat,[61] infrared reflectivity,[62] dc-Hall angle,[63–65] scanning tunneling microscopy (STM),[66] and ARPES measurements.[67]

Of particular interest, Corson *et al.* observed a similar phenomenon above T_c in both underdoped[68] and optimally[69] doped Bi-2212 in the longitudinal conductivity σ_{xx} using a terahertz spectroscopy technique. The real and imaginary part of σ_{xx} of underdoped Bi-2212 ($T_c=75$ K) as a function of temperature at 100 GHz $\sim$0.14 meV reveal that the ratio of the phase of the conductivity $\phi_{xx}=\mathrm{Im}(\sigma_{xx})/\mathrm{Re}(\sigma_{xx})$ at T_c to ϕ_{xx} at 100 K is $\gtrsim$4 indicating the imaginary part of σ_{xx} increases much more rapidly than the real part of σ_{xx} upon decreasing temperature toward T_c.[69] On optimally doped Bi-2212, only the real part of σ_{xx} as a function of temperature is reported where deviations away from the Drude (quasiparticle) contribution measured at frequencies 0.2, 0.6, and 0.8 THz is observed.[68] The magnitude of the conductivity enhancement above the Drude contribution is a factor of 2, 1.2, and 1.13, respectively, when temperature is reduced from 100 K to T_c.

From our transmission measurements as a continuous function of temperature analyzed in terms of a simple Drude response (reported in Ref. 33), we find an enhancement in the magnitude of the conductivity of 1.3 at 3.05 meV $\approx$0.7 THz and 1.1 at 5.24 meV$\approx$1.3 THz when the temperature is reduced from 100 K to T_c. The enhancement of the magnitude of the conductivity is expected to be larger than the enhancement of only the real part of the conductivity as measured by Corson *et al.* on optimally doped Bi-2212 due to the onset of a substantial imaginary part.

The precursive behavior observed in the IR Hall angle is definitively associated with the longitudinal channel and could possibly account for the entire behavior. Whether the off-axis conductivity contributes to the precursive behavior is not currently discernible.

IX. SUPERCONDUCTING STATE

To analyze the superconducting state, we use a variation in a phenomenological model of the magnetoconductivity

which well described the FIR low-temperature (<20 K) magneto-optical response of superconducting YBCO thin films.[70–73] The model conductivity used to describe the low-temperature magneto-optical data consists of the sum of four temperature-independent Lorentzian oscillators: two associated with vortex core excitations, one associated with the zero-frequency resonance of the superfluid, and one associated with the thermally excited nodal quasiparticles.

Unlike the previously reported data, the present study covers a wide range of temperature. However, it remains instructive to extrapolate this low-temperature model to higher temperatures. The temperature dependence of the nodal quasiparticle fraction and scattering rate have been measured in microwave experiments[74] whose functional form is incorporated into the model. All other parameters are assumed temperature independent.

We note that many parameters cannot realistically be assumed temperature independent. For example, the size of the vortex cores increase with temperature[75] which decrease the core level spacing. The pinning frequency depends strongly on temperature (for example, it is *a priori* known that the pinning force vanishes above the vortex glass melting temperature, ~70 K).

Regardless, the coarse features of the FIR Hall data are reproduced (although significant deviations which are discussed in detail in Ref. 33 notably exist) by the following minimum number of terms in the conductivity expressed in the circular basis: a zero-frequency superfluid resonance (London term), a cyclotron resonance associated with the nodal quasiparticles, and one finite frequency oscillator,

$$\sigma_{\pm} = \left[\frac{f_L}{-i\omega} + \frac{f_p}{-i(\omega \pm \omega_p) + \Gamma_p(t)} \right] \times (1 - f_n(t)) + \frac{f_n(t)}{-i(\omega \pm \omega_n) + \Gamma_n},$$

where $t = T/T_c$ is the normalized temperature, the nodal quasiparticle fraction and scattering rate are $f_n(t) = 1$ and $\Gamma_n(t) = 16.3 \text{ meV } t^{1.65}$ for $t > 1$, and $f_n(t) = t^2$ and $\Gamma_n(t) = 16.3 \text{ meV } t^4$ for $t < 1$, the cyclotron frequency of the nodal quasiparticles $\omega_n = 0.38$ meV, the fraction associated with the number of particles condensed in the superfluid $f_L = 0.45$, and the required finite-frequency oscillator parameters given by $f_p = 0.04$, $\omega_p = 4.4$ meV, and $\Gamma_p = 2.5$ meV.

The London term alone in the conductivity causes no Hall effect. The high frequency 21.75 meV data is well described by the quasiparticle cyclotron resonance term independent of other possible resonant terms, an observation which is consistent with previous measurements on optimally doped YBCO.[71] The low-frequency data is not well described without the presence of a finite-frequency chiral oscillator ~4.5 meV. This resonant energy is similar to STM measurements of the first excited state vortex core energy ~7 meV above the Fermi energy for optimally doped Bi-2212 and ~5.5 meV for YBCO.[76] The resonant feature is also similar to earlier magneto-optical measurements on YBCO of a holelike chiral oscillator at ~3 meV.[72,73]

X. CONCLUSION

Measurements of the IR Hall angle on optimally doped Bi-2212 were performed in fields up to 8 T as a continuous function of temperature at four discrete frequencies ranging from 3 to 22 meV. Above T_c, the IR Hall response characterized by ω_H is found to be significantly larger than the value calculated within a Boltzmann formalism using ARPES measured parameters. This is the THz manifestation of the well-known anomalous dc-Hall effect where dc-R_H enhancements are much larger than the value expected from Luttinger's theorem as well as the ARPES+RTA value. These enhancements as well as the frequency and temperature dependence of the dc- and IR Hall response is well described by a Fermi-liquid theory which incorporates the current vertex corrections produced by electron-electron interactions mediated by antiferromagnetic fluctuations.

There exists precursive superconductivity signatures in the measured IR Hall response and transmission well above T_c. The low-frequency data in the superconducting state requires a finite-frequency chiral oscillator ~4.5 meV in the conductivity, a resonance presumably associated with the vortex core states.

ACKNOWLEDGMENTS

This work was supported by the CNAM, NSF (Contract No. DMR-0030112), and DOE (Contract No. DE-AC02-98CH10886). The authors extend their thanks to Geoff Evans and Jeffrey R. Simpson for their assistance in performing the various reported measurements, Matthew Grayson for supplying the GaAs 2-DEG sample, and Andrea Damascelli and Giorgio Levy for providing ARPES Tl-2201 data.

[1] Z. Konstantinović, Z. Z. Li, and H. Raffy, Phys. Rev. B **62**, R11989 (2000).
[2] H.-C. Ri, R. Gross, F. Gollnik, A. Beck, R. P. Huebener, P. Wagner, and H. Adrian, Phys. Rev. B **50**, 3312 (1994).
[3] C. Kendziora, D. Mandrus, L. Mihaly, and L. Forro, Phys. Rev. B **46**, 14297 (1992).
[4] Z. Xu, J. Shen, S. Ooi, T. Mochiku, and K. Hirata, Physica C **421**, 61 (2005).
[5] J. M. Harris, Y. F. Yan, and N. P. Ong, Phys. Rev. B **46**, 14293 (1992).
[6] A. Damascelli, Z. Hussain, and Z.-X. Shen, Rev. Mod. Phys. **75**, 473 (2003).
[7] P. W. Anderson, *The Theory of Superconductivity in the High Tc Cuprates* (Princeton University Press, Princeton, NJ, 1997).
[8] C. M. Varma, P. B. Littlewood, S. Schmitt-Rink, E. Abrahams, and A. E. Ruckenstein, Phys. Rev. Lett. **63**, 1996 (1989).
[9] N. Doiron-Leyraud, C. Proust, D. LeBoeuf, J. Levallois, J.-B. Bonnemaison, R. Liang, D. A. Bonn, W. N. Hardy, and L. Taillefer, Nature (London) **447**, 565 (2007).
[10] E. A. Yelland, J. Singleton, C. H. Mielke, N. Harrison, F. F.

Balakirev, B. Dabrowski, and J. R. Cooper, Phys. Rev. Lett. **100**, 047003 (2008).
[11] A. F. Bangura *et al.*, Phys. Rev. Lett. **100**, 047004 (2008).
[12] C. Jaudet *et al.*, Phys. Rev. Lett. **100**, 187005 (2008).
[13] B. Vignolle, A. Carrington, R. A. Cooper, M. M. J. French, A. P. Mackenzie, C. Jaudet, D. Vignolles, C. Proust, and N. E. Hussey, Nature (London) **455**, 952 (2008).
[14] M. Platé *et al.*, Phys. Rev. Lett. **95**, 077001 (2005).
[15] M. Abdel-Jawad, M. P. Kennett, L. Balicas, A. Carrington, A. P. Mackenzie, R. H. Mckenzie, and N. E. Hussey, Nat. Phys. **2**, 821 (2006).
[16] A. P. Mackenzie, S. R. Julian, D. C. Sinclair, and C. T. Lin, Phys. Rev. B **53**, 5848 (1996).
[17] D. C. Peets, J. D. F. Mottershead, B. Wu, I. S. Elfimov, R. Liang, W. N. Hardy, D. A. Bonn, M. Raudsepp, N. J. C. Ingle, and A. Damascelli, New J. Phys. **9**, 28 (2007).
[18] D. J. Singh and W. E. Pickett, Physica C **203**, 193 (1992).
[19] C. Proust, E. Boaknin, R. W. Hill, L. Taillefer, and A. P. Mackenzie, Phys. Rev. Lett. **89**, 147003 (2002).
[20] A. Kanigel *et al.*, Nat. Phys. **2**, 447 (2006).
[21] L. Taillefer, J. Phys.: Condens. Matter **21**, 164212 (2009).
[22] L. B. Rigal, D. C. Schmadel, H. D. Drew, B. Maiorov, E. Osquiguil, J. S. Preston, R. Hughes, and G. D. Gu, Phys. Rev. Lett. **93**, 137002 (2004).
[23] W. J. Padilla, Y. S. Lee, M. Dumm, G. Blumberg, S. Ono, K. Segawa, S. Komiya, Y. Ando, and D. N. Basov, Phys. Rev. B **72**, 060511 (2005).
[24] T. Timusk and B. Statt, Rep. Prog. Phys. **62**, 61 (1999).
[25] H. F. Fong, B. Keimer, D. L. Milius, and I. A. Aksay, Phys. Rev. Lett. **78**, 713 (1997).
[26] G. S. Jenkins, D. C. Schmadel, P. L. Bach, R. L. Greene, X. Béchamp-Laganière, G. Roberge, P. Fournier, H. Kontani, and H. D. Drew, Phys. Rev. B **81**, 024508 (2010).
[27] H. Kontani, Rep. Prog. Phys. **71**, 026501 (2008).
[28] G. S. Jenkins, D. C. Schmadel, P. L. Bach, R. L. Greene, X. Béchamp-Laganière, G. Roberge, P. Fournier, and H. D. Drew, Phys. Rev. B **79**, 224525 (2009).
[29] S. R. Park, Y. S. Roh, Y. K. Yoon, C. S. Leem, J. H. Kim, B. J. Kim, H. Koh, H. Eisaki, N. P. Armitage, and C. Kim, Phys. Rev. B **75**, 060501(R) (2007).
[30] N. P. Armitage *et al.*, Phys. Rev. Lett. **88**, 257001 (2002).
[31] G. D. Gu, T. Egi, N. Koshizuka, P. A. Miles, G. J. Russell, and S. J. Kennedy, Physica C **263**, 180 (1996).
[32] G. S. Jenkins, D. C. Schmadel, and H. D. Drew, Rev. Sci. Instrum. **81**, 083903 (2010).
[33] G. S. Jenkins, Ph.D. thesis, University of Maryland, 2003.
[34] D. C. Schmadel, G. S. Jenkins, J. J. Tu, G. D. Gu, H. Kontani, and H. D. Drew, Phys. Rev. B **75**, 140506 (2007).
[35] D. C. Schmadel, Ph.D. thesis, University of Maryland, 2002.
[36] B. Parks, S. Spielman, and J. Orenstein, Phys. Rev. B **56**, 115 (1997).
[37] T. Valla, A. V. Fedorov, P. D. Johnson, B. O. Wells, S. L. Hulbert, Q. Li, G. D. Gu, and N. Koshizuka, Science **285**, 2110 (1999).
[38] A. Kaminski *et al.*, Phys. Rev. B **71**, 014517 (2005).
[39] Y.-D. Chuang, A. D. Gromko, A. V. Fedorov, Y. Aiura, K. Oka, Y. Ando, M. Lindroos, R. S. Markiewicz, A. Bansil, and D. S. Dessau, Phys. Rev. B **69**, 094515 (2004).
[40] T. Yamasaki, K. Yamazaki, A. Ino, M. Arita, H. Namatame, M. Taniguchi, A. Fujimori, Z.-X. Shen, M. Ishikado, and S. Uchida, Phys. Rev. B **75**, 140513 (2007).
[41] N. C. Plumb, T. J. Reber, J. D. Koralek, Z. Sun, J. F. Douglas, Y. Aiura, K. Oka, H. Eisaki, and D. S. Dessau, Phys. Rev. Lett. **105**, 046402 (2010).
[42] D. L. Feng *et al.*, Phys. Rev. Lett. **86**, 5550 (2001).
[43] J. D. Koralek *et al.*, Phys. Rev. Lett. **96**, 017005 (2006).
[44] Z.-X. Shen, and W.-S. Lee (private communication).
[45] A. A. Kordyuk, S. V. Borisenko, T. K. Kim, K. A. Nenkov, M. Knupfer, J. Fink, M. S. Golden, H. Berger, and R. Follath, Phys. Rev. Lett. **89**, 077003 (2002).
[46] M. A. Quijada, D. B. Tanner, R. J. Kelley, M. Onellion, H. Berger, and G. Margaritondo, Phys. Rev. B **60**, 14917 (1999).
[47] J. J. Tu, C. C. Homes, G. D. Gu, D. N. Basov, and M. Strongin, Phys. Rev. B **66**, 144514 (2002).
[48] A. J. Millis and H. D. Drew, Phys. Rev. B **67**, 214517 (2003).
[49] M. Grayson, L. B. Rigal, D. C. Schmadel, H. D. Drew, and P.-J. Kung, Phys. Rev. Lett. **89**, 037003 (2002).
[50] N. P. Ong, Phys. Rev. B **43**, 193 (1991).
[51] H. Matsui, T. Takahashi, T. Sato, K. Terashima, H. Ding, T. Uefuji, and K. Yamada, Phys. Rev. B **75**, 224514 (2007).
[52] J. Lin and A. J. Millis, Phys. Rev. B **72**, 214506 (2005).
[53] N. E. Hussey, M. Abdel-Jawad, A. Carrington, A. P. Mackenzie, and L. Balicas, Nature (London) **425**, 814 (2003).
[54] A. Damascelli and G. Levy (private communication).
[55] S. Ono, S. Komiya, and Y. Ando, Phys. Rev. B **75**, 024515 (2007).
[56] O. K. Andersen, A. I. Liechtenstein, O. Jepsen, and F. Paulsen, J. Phys. Chem. Solids **56**, 1573 (1995).
[57] A. J. Millis, A. Zimmers, R. P. S. M. Lobo, N. Bontemps, and C. C. Homes, Phys. Rev. B **72**, 224517 (2005).
[58] H. Kontani, K. Kanki, and K. Ueda, Phys. Rev. B **59**, 14723 (1999).
[59] S. Kamal, R. Liang, A. Hosseini, D. A. Bonn, and W. N. Hardy, Phys. Rev. B **58**, R8933 (1998).
[60] Y. Wang, Z. A. Xu, T. Kakeshita, S. Uchida, S. Ono, Y. Ando, and N. P. Ong, Phys. Rev. B **64**, 224519 (2001).
[61] J. W. Loram, J. L. Luo, J. R. Cooper, W. Y. Liang, and J. L. Tallon, Physica C **341-348**, 831 (2000).
[62] H. J. A. Molegraaf, C. Presura, D. van der Marel, P. H. Kes, and M. Li, Science **295**, 2239 (2002).
[63] D. Matthey, S. Gariglio, B. Giovannini, and J.-M. Triscone, Phys. Rev. B **64**, 024513 (2001).
[64] B. Bucher, P. Steiner, J. Karpinski, E. Kaldis, and P. Wachter, Phys. Rev. Lett. **70**, 2012 (1993).
[65] R. Jin and H. R. Ott, Phys. Rev. B **57**, 13872 (1998).
[66] C. Renner, B. Revaz, J.-Y. Genoud, K. Kadowaki, and O. Fischer, Phys. Rev. Lett. **80**, 149 (1998).
[67] M. R. Norman, M. Randeria, H. Ding, and J. C. Campuzano, Phys. Rev. B **57**, R11093 (1998).
[68] J. Corson, J. Orenstein, S. Oh, J. O'Donnell, and J. N. Eckstein, Phys. Rev. Lett. **85**, 2569 (2000).
[69] J. Corson, R. Mallozzi, J. Orenstein, J. N. Eckstein, and I. Bozovic, Nature (London) **398**, 221 (1999).
[70] S. G. Kaplan, S. Wu, H.-T. S. Lihn, H. D. Drew, Q. Li, D. B. Fenner, J. M. Phillips, and S. Y. Hou, Phys. Rev. Lett. **76**, 696 (1996).
[71] K. Karrai, E. Choi, F. Dunmore, S. Liu, X. Ying, Q. Li, T. Venkatesan, H. D. Drew, Q. Li, and D. B. Fenner, Phys. Rev. Lett. **69**, 355 (1992).
[72] S. Wu, Ph.D. thesis, University of Maryland, 1997.

[73] H.-T. S. Lihn, Ph.D. thesis, University of Maryland, 1996.
[74] D. A. Bonn *et al.*, Phys. Rev. B **47**, 11314 (1993).
[75] J. E. Sonier, R. F. Kiefl, J. H. Brewer, D. A. Bonn, S. R. Dunsiger, W. N. Hardy, R. Liang, R. I. Miller, D. R. Noakes, and C. E. Stronach, Phys. Rev. B **59**, R729 (1999).
[76] S. H. Pan, E. W. Hudson, A. K. Gupta, K.-W. Ng, H. Eisaki, S. Uchida, and J. C. Davis, Phys. Rev. Lett. **85**, 1536 (2000).